Article

C CPMAS Spectroscopy of Deuterated Proteins: CP Dynamics, Line Shapes, and *T* Relaxation

Corey R. Morcombe, Vadim Gaponenko, R. Andrew Byrd, and Kurt W. Zilm

J. Am. Chem. Soc., **2005**, 127 (1), 397-404• DOI: 10.1021/ja045581x • Publication Date (Web): 07 December 2004

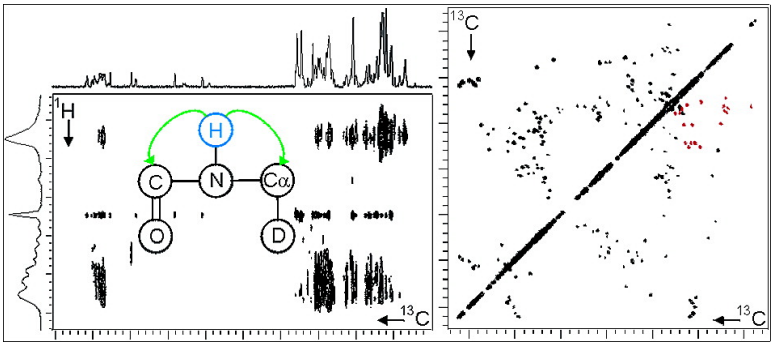

More About This Article

Additional resources and features associated with this article are available within the HTML version:

- Supporting Information
- Links to the 4 articles that cite this article, as of the time of this article download
- Access to high resolution figures
- Links to articles and content related to this article
- Copyright permission to reproduce figures and/or text from this article

View the Full Text HTML

J|A|C|S
ARTICLES
Published on Web 12/07/2004

^{13}C CPMAS Spectroscopy of Deuterated Proteins: CP Dynamics, Line Shapes, and T_1 Relaxation

Corey R. Morcombe,[†] Vadim Gaponenko,[‡] R. Andrew Byrd,[‡] and Kurt W. Zilm*,[†]

Contribution from the Department of Chemistry, Yale University, P.O. Box 208107, New Haven, Connecticut 06520-8107, and the Structural Biophysics Laboratory, National Cancer Institute, Frederick, Maryland 21702

Received July 22, 2004; E-mail: kurt.zilm@yale.edu

Abstract: ^{13}C CPMAS NMR has been investigated in application to protein samples with a variety of deuteration patterns. Samples were prepared with protons in either all hydrogen positions, only in the exchangeable sites, or in the exchangeable sites plus select methyl groups. CP dynamics, T_1 relaxation times, and ^{13}C line widths have been compared. Using ubiquitin as a model system, reasonable ^{1}H−^{13}C CP transfer is observed for the extensively deuterated samples. In the absence of deuterium decoupling, the ^{13}C line widths observed for the deuterated samples are identical to those observed for the perprotio samples with a MAS rate of 20 kHz. Extensive deuteration has little effect on the T_1 of the exchangeable protons. On the basis of these observations, it is clear that there are no substantive compromises accompanying the use of extensive deuteration in the design of ^{1}H, ^{15}N, or ^{13}C solid-state NMR methods.

Introduction

Deuteration has played a significant role in solution NMR of proteins. Short transverse relaxation times T_2 limit the spectral resolution in studies of large proteins with long correlation times. ^{1}H−^{1}H dipolar mediated relaxation is often a significant fraction of these transverse relaxation rates and can largely be eliminated by extensive deuteration. As reviewed by Gardner and Kay,[1] deuteration of all nonexchangeable ^{1}H's to a level of 80−90% increases ^{1}H T_2's by approximately 2-fold over those observed in perprotio proteins, i.e., proteins containing ^{1}H's at natural abundance. Deuteration also provides the added benefit of suppressing J_{HH} scalar couplings, further improving spectral resolution. Since solution NMR of macromolecular systems nearly always uses ^{1}H detection, this results in concomitant increases in sensitivity as well as resolution.

In solid-state NMR (ssNMR), deuteration has been used to dilute ^{1}H's to eliminate the strong ^{1}H homonuclear dipolar couplings, resulting in narrow ^{1}H lines without the need for multiple pulse ^{1}H homonuclear decoupling.[2] Studies have been done on both deuterated peptides[3] and deuterated proteins,[4] including recent work where direct detection of ^{1}H's was successfully employed to acquire ^{1}H−^{15}N correlation spectra of deuterated proteins.[5,6] While ^{1}H experiments using magnetic dilution do provide many new avenues to obtain structural information[4] by ssNMR, it is not generally possible to make the required resonance assignments from ^{1}H and ^{15}N experiments alone.

Sequential backbone assignments are most straightforward if the CO and Cα ^{13}C resonances are used. Backbone walks of proteins in the solid state have been demonstrated by NCOCA and NCACX experiments.[7,8] ^{13}C spectra are also key for spin system identification, and side chain assignments[9] can be critical for identifying long-range tertiary contacts. The complementary information obtained from NCACX experiments and 2-D ^{13}C−^{13}C correlation experiments can be combined to provide full sets of assignments with great confidence.[9−14]

Several potential problems arise in combining ^{13}C based assignment experiments with ^{1}H ssNMR structural studies using magnetic dilution. In extensively deuterated samples, the resonances for ^{13}C centers bonded to ^{2}H experience sizable isotope shifts.[15] These shifts complicate the transfer of ^{13}C resonance assignments from a perprotio sample directly to spectra acquired for perdeuterated protein. It is then preferable and more convenient to perform ^{1}H and ^{13}C measurements on

[†] Yale University.
[‡] National Cancer Institute.

(1) Gardner, K. H.; Kay, L. E. *Ann. Rev. Biophys. Biomol. Struct.* **1998**, *27*, 357−406.
(2) McDermott, A. E.; Creuzet, F. J.; Kolbert, A. C.; Griffin, R. G. *J. Magn. Reson.* **1992**, *98*, 408−413.
(3) Reif, B.; Griffin, R. G. *J. Magn. Reson.* **2003**, *160*, 78−83.
(4) Paulson, E. K.; Morcombe, C. R.; Gaponenko, V.; Dancheck, B.; Byrd, R. A.; Zilm, K. W. *J. Am. Chem. Soc.* **2003**, *125*, 14222−14223.
(5) Chevelkov, V.; van Rossum, B. J.; Castellani, F.; Rehbein, K.; Diehl, A.; Hohwy, M.; Steuernagel, S.; Engelke, F.; Oschkinat, H.; Reif, B. *J. Am. Chem. Soc.* **2003**, *125*, 7788−7789.
(6) Paulson, E. K.; Morcombe, C. R.; Gaponenko, V.; Dancheck, B.; Byrd, R. A.; Zilm, K. W. *J. Am. Chem. Soc.* **2003**, *125*, 15831−15836.
(7) Straus, S. K.; Bremi, T.; Ernst, R. R. *J. Biomol. NMR* **1998**, *12*, 39−50.
(8) Hong, M. *J. Biomol. NMR* **1999**, *15*, 1−14.
(9) McDermott, A.; Polenova, T.; Bockmann, A.; Zilm, K. W.; Paulsen, E. K.; Martin, R. W.; Montelione, G. T. *J. Biomol. NMR* **2000**, *16*, 209−219.
(10) Pauli, J.; Baldus, M.; van Rossum, B.; de Groot, H.; Oschkinat, H. *ChemBioChem* **2001**, *2*, 272−281.
(11) Pauli, J.; van Rossum, B.; Forster, H.; de Groot, H. J. M.; Oschkinat, H. *J. Magn. Reson.* **2000**, *143*, 411−416.
(12) Bockmann, A.; Lange, A.; Galinier, A.; Luca, S.; Giraud, N.; Juy, M.; Heise, H.; Montserret, R.; Penin, F.; Baldus, M. *J. Biomol. NMR* **2003**, *27*, 323−339.
(13) Igumenova, T. I.; McDermott, A. E.; Zilm, K. W.; Martin, R. W.; Paulson, E. K.; Wand, A. J. *J. Am. Chem. Soc.* **2004**, *126*, 6720−6727.
(14) Igumenova, T. I.; Wand, A. J.; McDermott, A. E. *J. Am. Chem. Soc.* **2004**, *126*, 5323−5331.
(15) Gardner, K. H.; Rosen, M. K.; Kay, L. E. *Biochemistry* **1997**, *36*, 1389−1401.

the same deuterated sample. One might however expect ^{13}C cross polarization (CP) magic-angle spinning (MAS) NMR of deuterated proteins to present several new difficulties. By diluting the ^{1}H pool there is less ^{1}H magnetization available for CP, and therefore the ultimate enhancement of the ^{13}C signal will be lessened. Diluting the ^{1}H bath would also be expected to increase the ^{1}H T_1 time, requiring the recycle delay to be lengthened in any ^{13}C or ^{15}N observed CPMAS experiments. In addition to these potential losses in sensitivity, it might also be expected that ^{2}H decoupling[16] would be needed to maintain high resolution in the ^{13}C spectra of deuterated sites. $^{1}H/^{15}N/^{13}C$ triple resonance experiments would then require a more complex four-channel CPMAS probe.

In this report we demonstrate that these potential drawbacks do not in fact present any significant difficulties to ^{13}C CPMAS spectroscopy of heavily deuterated proteins. Reasonable CP efficiency is obtained for CO and Cα carbons in deuterated samples. When select perprotio methyl groups are incorporated into the sample, good CP transfer to the majority of side chain carbons is also observed. Deuteration has surprisingly little effect on both ^{1}H and ^{13}C longitudinal relaxation times. A comparison of ^{1}H decoupled ^{13}C line widths for Cα carbons in perprotio and perdeutero ubiquitin finds no statistically significant differences, and therefore deuterium decoupling is not a strict requirement. It is also observed that ^{1}H decoupling can be dispensed with as well when observing deuterated ^{13}C centers if a modest 12% increase in line width can be tolerated. Taken together these observations indicate that application of the entire suite of resonance assignment techniques to extensively deuterated protein samples should be straightforward.

Materials and Methods

Samples. All nanocrystalline ubiquitin samples studied were precipitated using 2-methyl-2,4,-pentanediol (MPD) as described elsewhere.[13] Perdeuterated MPD was used to prepare all deuterated samples. Ubiquitin with no isotopic enrichment (Sigma) was crystallized without further purification and is denoted n-ubq (normal ubiquitin). The extensively deuterated samples include ND-ubq, a uniformly ^{15}N and ^{2}H enriched ubiquitin sample, and ilvD-ubq, a sample uniformly enriched in ^{2}H, ^{13}C, and ^{15}N, but also incorporating perprotio methyl groups in all leucines and valines, and at the δ-1 position of all isoleucines[17](ilv-methyls). Both the ND-ubq and ilvD-ubq samples had all their labile protons exchanged in normal water prior to crystallization. Deuterium incorporation in all cases was better than 95% as determined by mass spectrometry. Two ^{13}C and ^{15}N enriched samples with perprotio side chains were used for comparison. The first sample was a 50/50 mixture of uniformly $^{13}C/^{15}N$ enriched ubiquitin and n-ubq and is denoted as CN-ubq. The second was a lyophilized sample of uniformly ^{13}C and ^{15}N enriched ubiquitin, referred to as CN2-ubq.

NMR Spectroscopy. All data were acquired on a Varian Inova 800 MHz NMR spectrometer using a home-built triple resonance $^{1}H/^{13}C/^{15}N$ CPMAS probe[18] employing 2.5 mm rotors with a sample volume of 6.5 μL. Unless otherwise stated the MAS rate was set to 20 kHz, the sample temperature held close to 10 °C, and CP performed at the $\omega_1^H - \omega_1^X = \omega_r$ matching condition. Other pertinent experimental details are included in the figure captions.

(16) Grzesiek, S.; Anglister, J.; Ren, H.; Bax, A. *J. Am. Chem. Soc.* **1993**, *115*, 4369−4370.
(17) Goto, N. K.; Gardner, K. H.; Mueller, G. A.; Willis, R. C.; Kay, L. E. *J. Biomol. NMR* **1999**, *13*, 369−374.
(18) Martin, R. W.; Paulson, E. K.; Zilm, K. W. *Rev. Sci. Instrum.* **2003**, *74*, 3045−3061.

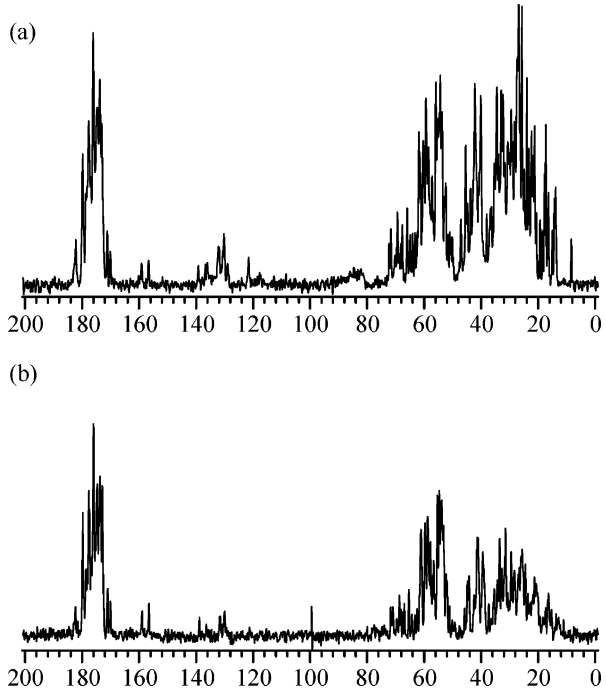

Figure 1. Natural abundance ^{13}C CPMAS spectra of (a) n-ubq and (b) ND-ubq nanocrystals. In the case of the ND-ubq sample the MPD precipitant was also perdeuterated. The spectra were signal averaged for 30 000 scans using a 2 s recycle delay and a MAS rate $\omega_r/2\pi = 20$ kHz. The CP contact time was 1.8 ms in part a and 2.5 ms in part b. In all experiments the ^{13}C CP power level was set to provide a ^{13}C radio frequency field amplitude of $\omega_1^C/2\pi = 80$ kHz, and the ^{1}H field was matched to $\omega_1^H/2\pi = 100$ kHz. TPPM decoupling was employed at $\omega_1^H/2\pi = 115$ kHz in part a and 95 kHz in part b. Both spectra were apodized with identical cosine bells.

Comparison of CP Dynamics

Figure 1 demonstrates CP is readily applied to a perdeuterated ubiquitin sample. The spectrum shown in Figure 1a is for n-ubq, the sample with no isotopic enrichment. With the full complement of protons present, the CP enhancement of the natural abundance ^{13}C CPMAS spectrum is very reasonable. The spectrum shown in Figure 1b is for the ND-ubq sample. The ^{1}H magnetization transferred to the natural abundance ^{13}C comes primarily from the exchanged amide sites, and to a much lesser extent the water present within the crystals (vide infra). Since the two samples contain close to the same volume of protein nanocrystals, the relative intensities give an estimate of the reduction in CP efficiency obtained for the heavily deuterated sample. The carbonyl region (170−185 ppm) is 70% as intense, while the primarily Cα region (45−75 ppm) is 62% as intense for the ND-ubq sample as for the n-ubq sample. This is consistent with the picture that these two types of carbon sites receive the majority of their magnetization from the amide protons. On the other hand the remaining side chain region from 8 to 45 ppm is only 40% as intense. Since this portion of the spectrum contains the resonances including the more hydrophobic groups that are situated further from the amides and away from any crystal water, this is to be expected. The observation that the important CO and Cα regions for the deuterated sample are down only by $\sim^1/_3$ in comparison to the n-ubq sample makes it clear that ^{13}C sensitivity is not sacrificed as much as might be estimated solely on the basis of relative proton content. Considering only the protein, the H/C ratio is ∼1.71 for the n-ubq sample, while it is only ∼0.42 for ND-ubq.

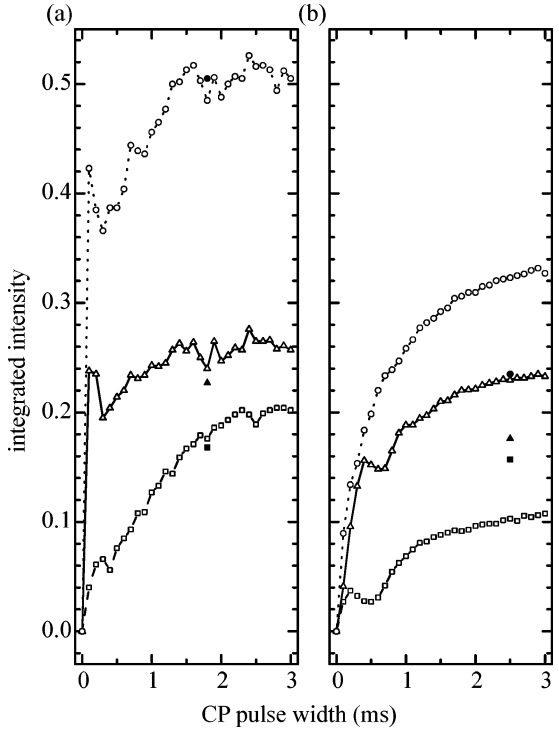

Figure 2. ^{1}H to ^{13}C contact time plots for (a) CN-ubq and (b) ilvD-ubq. The contact time was linearly varied from 0.1 to 3.0 ms in steps of 100 μs. The squares and dashed line plot the integrals of the region of the spectrum from 165 to 185 ppm, containing the CO resonances. The triangles and solid line plot the integrals of the primarily Cα region from 45 to 75 ppm. Circles and a dotted line plot the integrals for the remaining side chain peaks. The total magnetization normalized for unit intensity at 3 ms in parts a and b is scaled by the relative CP enhancement. The solid symbols indicate where the corresponding integrals fall for the n-ubq and the ND-ubq data shown in Figure 1. These were scaled so that the total n-ubq magnetization was the same as that for the CN-ubq sample at the same contact time.

Overall the spectra in Figure 1 are quite similar in the CO and Cα bands. There are minor differences in resolution, primarily in the CO region of the spectrum. Resolution here is quite sensitive to sample quality and how carefully the TPPM decoupling[19] parameters are optimized, and we would not attribute any of these differences to being solely a consequence of deuteration.

To better characterize differences between the CP dynamics of perprotio and extensively deuterated samples, CP buildup curves at the MAS rate of 20 kHz were acquired for two of the samples uniformly enriched in ^{13}C. A constant level CP sequence was used, taking precautions we have described before[6,18,20] to ensure that radio frequency (RF) field inhomogeniety effects do not dominate the results under fast MAS conditions. The first sample used was CN-ubq, the 50/50 mixture of uniformly ^{13}C/^{15}N enriched ubiquitin and n-ubq, and the second sample used was the ilvD-ubq sample. Both have protons in the amide and other exchangeable positions, while the ilvD-ubq has additional methyl group protons. The H/C ratio in ilvD-ubq is ∼60% greater than that for ND-ubq but, at 0.69, is still much less than the 1.71 for n-ubq.

The results for the CN-ubq sample are shown in Figure 2a. In each spectrum the CO, Cα, and side chain regions were integrated separately and plotted versus the contact time. The Cα ^{13}C resonances in the CN-ubq sample polarize very rapidly, principally exchanging magnetization with their α-protons. The intensity after a 100 μs contact time is nearly as high as that after 3 ms of CP. The carbonyls also display a slight CP transient oscillation, which is likely to be due to CP with the amide protons. The much slower additional long term buildup of the carbonyl intensity is characteristic of a carbon center without a directly attached hydrogen being cross polarized simultaneously by several distant protons.

Figure 2b contrasts these results to those for the ilvD-ubq sample. These data were scaled relative to the CN-ubq plot using the relative CP enhancements measured in a ^{13}C inversion recovery T_1 experiment that will be described shortly. Both the carbonyl and Cα bands display slight transient CP oscillations. These now occur at a longer time and are most likely a result of the initial CP being dominated by the nearby amide protons. Overall all three regions of the spectrum build more slowly, again indicative that CP involves many protons either directly or indirectly via ^{1}H spin diffusion. In comparison to the ND-ubq sample the Cα and side chain resonances are significantly more intense due to the extra ^{1}H magnetization available in the perprotio ilv-methyls. The CO intensity is observed to be somewhat less than ultimately achieved in the ND-ubq sample. These intensities taken from the spectra in Figure 1 are also included in the plots shown in Figure 2. This difference in part is a result of the fact that the CP matching condition for the CO band is found to be very sensitive in any of the perdeuterated samples, while the Cα band is less sensitive to the match. In the uniformly ^{13}C enriched ilvD-ubq sample the CO carbons also always have to compete with a neighboring Cα carbon for the amide proton magnetization. In the n-ubq and ND-ubq samples this is not a factor as the ^{13}C is at natural abundance.

Some insight into exactly which protons contribute to CP of the different types of ^{13}C centers can be obtained from ^{1}H−^{13}C correlation spectra. This also provides an experimental probe of the potential role of bound water in the CP dynamics not considered in the above discussion. A pair of ^{1}H−^{13}C correlation spectra for the ilvD-ubq sample were acquired at contact times of 200 μs and 2 ms using ^{13}C detection and are shown in Figure 3 using the pulse sequence described in Figure 4a. Only MAS was used for ^{1}H line narrowing, and no decoupling was applied to the ^{13}C during t_1. The ^{1}H chemical shift dimension cleanly separates into three distinct regions. The ilv-methyls resonate in a 2 ppm wide band centered at ∼1 ppm; water, serine hydroxyls, and threonine hydroxyls resonate at ∼5 ppm; while the remaining exchangeable protons span a band from 6 to 11 ppm. Integrating the intensity of the CO, Cα, and side chain regions correlated with these three ^{1}H chemical shift regions shows that little of the ^{1}H magnetization in the water ever makes it into the ^{13}C via CP. In the 200 μs spectrum the side chain carbons correlate strongly with the methyl ^{1}H's, while the CO and Cα carbons are correlated principally to the amide protons. The net ^{13}C CP signal at the 200 μs contact time originates from ^{1}H magnetization that is 37% ilv-methyl and 61% amide. Only 2% comes from the protons at 5 ppm, which on the basis of the receiving ^{13}C chemical shifts can be assigned solely to serine and threonine hydroxyl ^{1}H magnetization. During the 2 ms contact time in the second experiment ^{1}H spin diffusion thoroughly mixes the ^{1}H pool, and all ^{13}C shifts are significantly

(19) Bennett, A. E.; Rienstra, C. M.; Auger, M.; Lakshmi, K. V.; Griffin, R. G. *J. Chem. Phys.* **1995**, *103*, 6951−6958.
(20) Paulson, E. K.; Zilm, K. W. *J. Magn. Reson.* **2004**, submitted for publication.

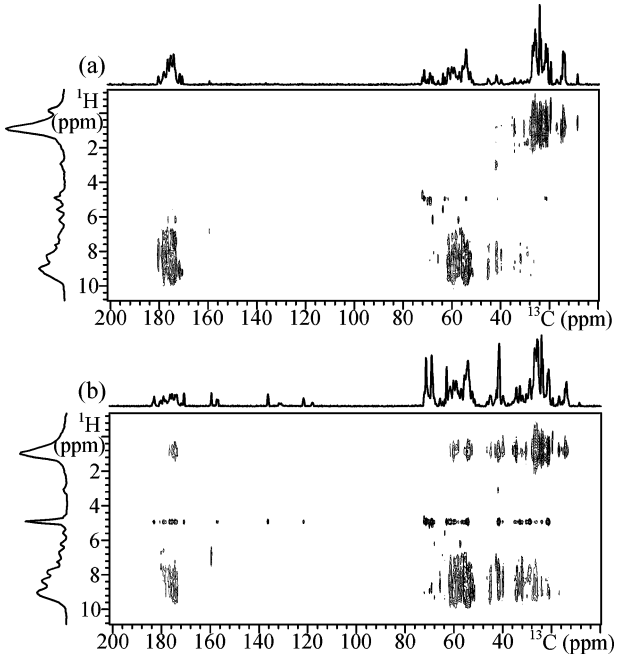

Figure 3. ^{1}H−^{13}C correlation spectra of ilvD-ubq. The spectra were taken with (a) 0.2 ms and (b) 2 ms CP contact times, using the pulse sequence shown in Figure 4a. Each spectrum contains 128 t_1 increments (real + imaginary), with 140 scans per increment, totalling 10 h. All dimensions were apodized with cosine bell functions.

correlated to all three types of ^{1}H. The ^{13}C chemical shifts can no longer be used to identify the 5 ppm ^{1}H band solely with side chain hydroxyls. Since it is also known that the amide ^{1}H bath cross relaxes with the larger water pool[4] at a rate of 90 s^{-1}, we assign ^{13}C intensity coming from ^{1}H signal at 5 ppm in the 2 ms CP experiment as having largely originated with water. The partitioning of the ^{1}H magnetization contributing to the net CP signal in this experiment is 34% methyl, 54% amide, and 12% water. The lesser ultimate CP enhancement observed for ND-ubq is consistent with the absence of the 34% of magnetization that originates from the ilv-methyl groups in the ilvD-ubq sample. A breakdown of the how the ^{1}H magnetization at the two contact times partitions into the three ^{13}C resonance bands is provided in Table 1. These numbers show that the Cα and CO carbons still receive the majority of their polarization from the amide protons, while the ilv-methyls provide the majority for the side chain signals even at long contact times.

CP Enhancements and Effects of Deuteration on T_1. The effects of deuteration on the ultimate CP enhancement factors and ^{13}C T_1 values are most easily measured by a CPMAS inversion recovery experiment. After the CP interval the ^{13}C magnetization is flipped down along the $-z$ axis, and the relaxation to thermal equilibrium followed by reading out the ^{13}C signal after a variable relaxation delay with a single $\pi/2$ pulse. The CP enhancement factor then is simply $-M(0)/M(\infty)$. Data acquired for the ilvD-ubq sample and the lyophilized CN2-ubq sample are shown in Figure 5. The CN2-ubq sample was used in place of the original CN-ubq sample after it was inadvertently and irreversibly damaged by too long of a ^{1}H decoupling pulse. In the ilvD-ubq sample the CP enhancements are found to be 0.54, 1.23, and 0.81 for the CO, Cα, and side chain regions, respectively. The corresponding numbers for the CN2-ubq sample are 1.11, 1.31, and 1.35. The average CP

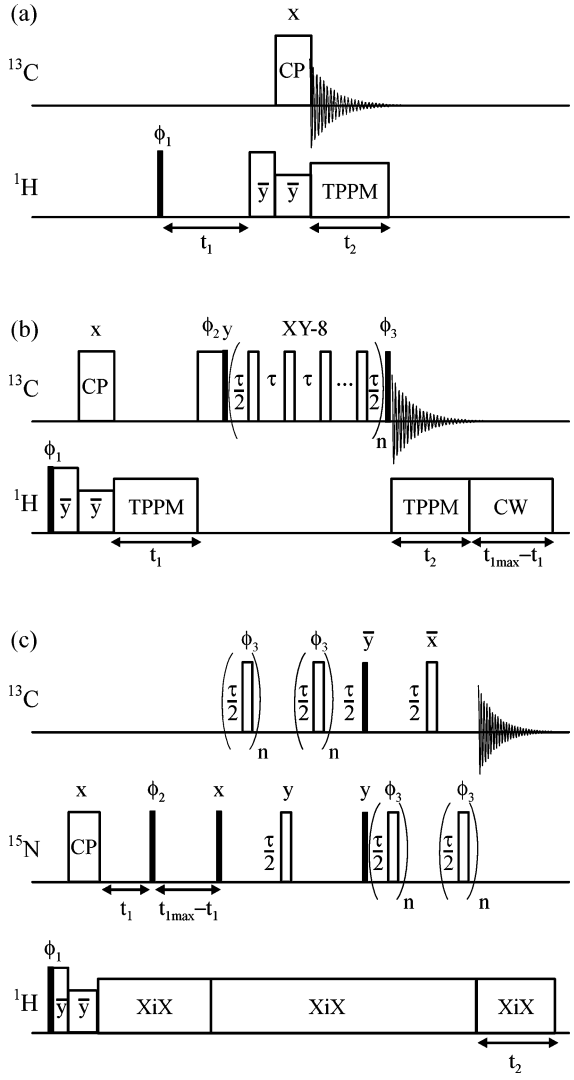

Figure 4. Pulse sequences used in this work. ^{13}C RF is applied to have an effective $\omega_1^C/2\pi = 89$ kHz, and ^{15}N RF to have an effective $\omega_1^N/2\pi = 55$ kHz throughout all experiments. ^{1}H RF is applied to have an effective $\omega_1^H/2\pi = 125$ kHz for short pulses, $\omega_1^H/2\pi = 100$ kHz for decoupling (XiX or TPPM), and matched to the $\omega_1^H - \omega_1^X = \omega_r$ matching condition during cross polarization periods. A ^{1}H spinlock pulse of 10 μs is applied prior to the initial CP pulses to avoid a timing delay associated with simultaneously changing the RF power level and phase. Solid bars represent $\pi/2$ pulses, open bars represent π pulses, and τ is one rotor period. (a) Two-dimensional ^{1}H−^{13}C correlation pulse sequence. Phase cycling of the receiver and $\phi_1 = x, -x$. States quadrature information was obtained by additional phase cycling of ϕ_1. (b) Two-dimensional ^{13}C homonuclear RFDR pulse sequence. A ^{13}C spinlock of 104 μs is performed at the end of the t_1 period. n was set to 4 sets of π pulses following an XY-8 phase cycle, totaling 1.6 ms of mixing. Phase cycling was as follows: $\phi_1 = x,x,x,x,-x,-x,-x,-x$; $\phi_2 = x,x,-x,-x,x,x,-x,-x$; $\phi_3 = x,-x,x,-x,x,-x,x,-x$; receiver $= x,-x,x,-x,x,-x,x,-x$. TPPI quadrature was obtained by advancing ϕ_2. (c) Two-dimensional ^{15}N−^{13}C correlation pulse sequence. The ^{1}H−^{15}N CP pulse is applied for 150 μs. Phase cycling of the receiver and $\phi_1 = x,-x$. $\phi_2 = -x$ and is alternated to collect States quadrature information. n is 11, and ϕ_1 is alternated in an XY-4 fashion, in this case starting and ending with a pulse of phase x.

enhancement is 0.86 for ilvD-ubq, 68% of the 1.26 average enhancement observed for CN2-ubq.

The ^{13}C T_1 values have also been extracted from these data. For both samples, the CO and Cα recovery curves fit single exponentials, while double exponentials were required to produce as good a fit for the side chain data. In the perprotio CN2-ubq sample the CO T_1 is found to be 3.55 s, while the Cα

Table 1. Fraction of ^{13}C CP Signal from Different ^{1}H Pools

experiment → / ^{1}H source ↓	CO 200 μs	Cα 200 μs	sc[a] 200 μs	CO 2 ms	Cα 2 ms	sc[a] 2 ms
amide	100	90	17	58	69	34
ilv-methyl	0	0	83	25	18	58
water				17	13	8
OH	0	10	0			

[a] sc = side chain carbon atoms, those with ^{13}C chemical shifts in the range of 8−45 ppm.

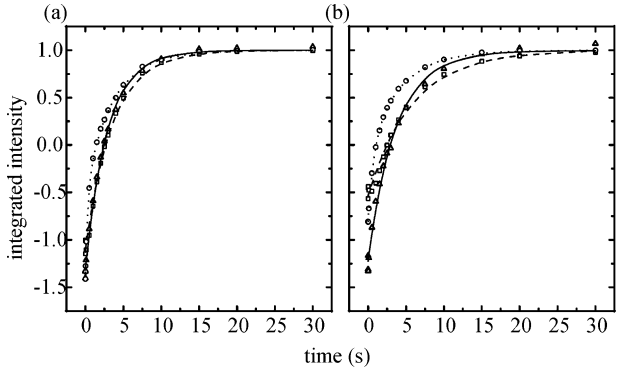

Figure 5. Inversion recovery data plotted for (a) lyophilized CN-ubq and (b) ilvD-ubq. A 2 ms contact time was used for both experiments prior to flipping the ^{13}C magnetization to the $-z$ axis. The squares and dashed line plot the integrals of the CO resonances. The triangles and solid line plot the integrals of the Cα peaks. These data were fit using nonlinear least squares to $M(t) = (M(0) - M(\infty))e^{t/T_1} + M(\infty)$, and the data normalized to set $M(\infty) = 1$. The circles and dotted line plot the integrals of the side chain peaks. These data were fit a double exponential of the form $M(t) = (M(0) - M(\infty))(ae^{t/T_{1a}} - (1 - a)e^{t/T_{1b}}) + M(\infty)$.

T_1 is shorter at 2.88 s. Deuteration produces only a modest increase in these relaxation times, with the CO and Cα T_1's being measured at 5.75 and 3.63 s, respectively, in the ilvD-ubq sample. The double exponential fits for the side chain resonances are quite interesting. In both samples the longer T_1 accounts for ∼60% of the magnetization, while a much shorter T_1 is required for the recovery of the remaining 40%. The side chain ^{13}C resonances for the perprotio CN2-ubq sample fit a double exponential with 63% at a T_1 of 3.56 s and 37% displaying a T_1 of 0.27 s. In the ilvD-ubq data the fit finds 62% having a T_1 of 4.04 s, and 38% had an apparent T_1 of 0.64 s.

In all cases the relaxation times of the ^{13}Cs were lengthened by deuteration yet remain shorter than typically observed in model organic solids. The average ^{1}H T_1's of these samples are also quite short, measured at 0.3−0.4 s for n-ubq and ND-ubq and 0.2 s for the ilvD-ubq sample. The observation that deuteration of all methyls in the ND-ubq sample does not lengthen the ^{1}H T_1 time would indicate that these relatively short ^{1}H T_1 values are not due to rotating methyl groups acting directly as relaxation sinks. The double exponential ^{13}C T_1 relaxation for the side chain resonances is however consistent with the presence of some sort of relaxation sink giving rise to the very short ^{13}C T_1 observed for the rapidly relaxing fraction. One possible explanation is spin diffusion-limited paramagnetic relaxation caused by molecular oxygen. Since oxygen is much more soluble in hydrophobic than hydrophilic environments,[21] it would be expected that these ^{13}C spins would be the most dramatically impacted. Spin diffusion among the isotopically enriched ^{13}C then helps to relax the more distant ^{13}C sites. Experiments are in progress to test this hypothesis.

Table 2. Signal Intensities for Spectra in Figure 6

experiment	sc[a] integral	Cα integral	CO integral	total integral
Bloch decay	0.52	0.22	0.26	1.00
2 ms CP	0.39	0.23	0.15	0.77
spinlock-CP	0.60	0.29	0.20	1.09
NOP	0.41	0.09	0.14	0.64
RADCP	0.57	0.27	0.23	1.07

[a] sc = side chain carbon atoms, those with ^{13}C chemical shifts in the range of 8−45 ppm.

Given the CP enhancements are small and that the ^{13}C relaxation times are short, a significant gain in sensitivity should be possible by using the ^{13}C z-magnetization M_z^C present prior to CP, especially for the ilvD-ubq sample. Figure 6 contains a comparison of the signal obtained in (a) a Bloch decay with a 20 s relaxation delay to (b) a CP spectrum using a 2 s relaxation delay and to (c) the CP result obtained with M_z^C being spinlocked prior to the CP interval. While the standard CP spectrum is only 77% of the intensity of the Bloch decay, the spinlock CP is 109% as intense. The presence of the ilv-methyl groups in this sample also makes it possible to apply the NOP-MAS or nuclear Overhauser polarization-MAS experiment.[22] In this technique the ^{13}C is polarized by saturating the protons to produce a nuclear Overhauser effect, and the saturating ^{1}H RF is applied at a level to match the MAS rate. This latter condition also enhances ^{13}C−^{13}C spin diffusion in an attempt to redistribute the ^{13}C polarization more evenly among all the ^{13}C nuclei. The spectrum in Figure 6d was obtained in this manner with a 2 s relaxation delay. While the side chain signal obtained is 79% of the equilibrium magnetization observed in the Bloch decay, the COs only rise to 54%, and the Cα's, to 41% of their thermal equilibrium polarizations. Although the NOP method has been shown to provide performance superior to CP on a lyophilized protein sample, it apparently provides no advantage in application to the samples studied here.

The final spectrum combines spinlock CP with the RF assisted diffusion CP or RADCP[23] technique. In RADCP the ^{13}C magnetization is immediately flipped back up along the $+z$ axis after creation by CP. As in the NOP-MAS method the ^{13}C magnetization is equilibrated among all the ^{13}C centers by ^{13}C−^{13}C spin exchange, again enhanced by application of a ^{1}H RF field matched to the MAS rate. After a RAD mixing period of ∼100 ms the ^{13}C signal is read out by a $\pi/2$ pulse. As seen in Figure 6e this spectrum has signals with relative intensities much closer to what is obtained in the fully relaxed Bloch decay spectrum, albeit in a much shorter time. As detailed in Table 2, the resulting total signal intensity is within experimental error the same as in the spinlock-CP spectrum, but the distribution of intensities is much closer to that obtained in the fully relaxed Bloch decay spectrum. For this nanocrystalline protein sample the spinlock-RADCP sequence provides the best combination of high signal-to-noise and quantitative signal response.

^{13}C Resolution of Deuterated ^{13}C Sites. Comparison of the ^{13}C line widths obtained with a deuterated sample to those

(21) Prosser, R. S.; Luchette, P. A.; Westerman, P. W.; Rozek, A.; Hancock, R. E. W. *Biophys. J.* **2001**, *80*, 1406−1416.

(22) Katoh, E.; Takegoshi, K.; Terao, T. *J. Am. Chem. Soc.* **2004**, *126*, 3653−3657.

(23) Morcombe, C. R.; Gaponenko, V.; Byrd, R. A.; Zilm, K. W. *J. Am. Chem. Soc.* **2004**, *126*, 7196−7197.

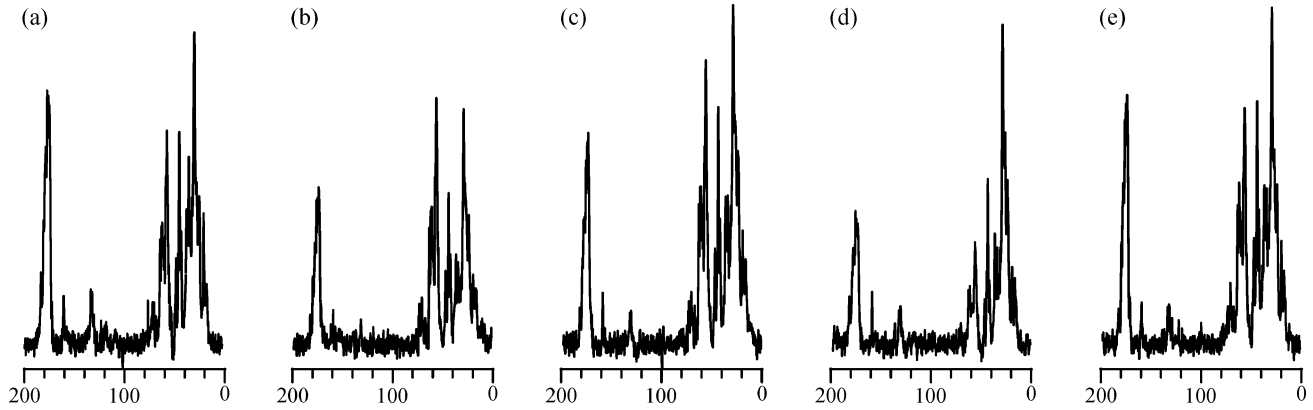

Figure 6. ^{13}C spectra of ilvD-ubq obtained using various ^{1}H polarization transfer schemes. Four scans were averaged in each, and the spectra were apodized with 50 Hz exponential decay functions. The recycle delay between successive scans was 2 s, with the exception of the Bloch decay spectrum (a) where it was set to 20 s. (b) CP spectrum taken with a 2 ms contact time. (c) 2 ms contact CP spectrum enhanced by spinlocking the ^{13}C magnetization present prior to the CP interval. In part d the ^{1}H's are saturated by applying a RF field set to $\omega_1^H/2\pi = 20$ kHz to produce an NOE to enhancement of the ^{13}C magnetization. Part e is taken by spinlocking the ^{13}C z-magnetization prior to CP as in part c, placing the ^{13}C magnetization back along the z-axis for 100 ms of RAD mixing and then finally reading out the signal with a ^{13}C $\pi/2$ pulse.

observed for a perprotio sample is most readily accomplished using two-dimensional ^{13}C−^{13}C and ^{15}N−^{13}C correlation spectroscopy. Using the ilvD-ubq sample, ^{13}C−^{13}C maps were taken using the RFDR recoupling sequence[24] implemented as diagramed in Figure 4b. Figure 7a shows the Cα and side chain region of the ^{1}H decoupled RFDR spectrum showing predominantly one bond correlations. In Figure 7b the ^{1}H decoupling was turned off during t_1, preferentially broadening the ilv-methyl group resonances in ω_1. Cross-peaks resulting as transfer of magnetization from these methyls are not observed, while those representing transfer to these methyls are. One can also see that the diagonal is broadened around 25 ppm because the leucine methyl resonances are concentrated in this region of the spectrum. Otherwise, the Cα−Cβ cross-peaks appear relatively unaffected by the elimination of ^{1}H decoupling.

To more quantitatively assess the Cα and CO ^{13}C line widths in the ilvD-ubq sample, ^{13}C detected ^{15}N-^{13}C correlation spectra were acquired. The pulse sequence used is shown in Figure 4c. ^{15}N coherence is created by a 150 μs ^{1}H to ^{15}N CP, ^{15}N chemical shift evolution occurs under 100 kHz XiX ^{1}H decoupling,[25] and the magnetization is transferred to ^{13}C using 4 ms of TEDOR.[26] The ^{13}C signal was observed both with and without 100 kHz of XiX ^{1}H decoupling during t_2. A set of 19 Cα and 31 CO peaks were chosen that were cleanly baseline resolved in both data sets. The distributions of line widths measured as full widths at half-maximum are depicted in Figure 8. In each case the arithmetic mean line width and the maximum of a fit to a Gaussian distribution agree to within 2 Hz. For the Cα peaks in the ilvD-ubq sample, average line widths with and without ^{1}H decoupling are found to be 116 Hz (0.58 ppm) and 131 Hz (0.65 ppm), respectively. The CO line widths are found to be 110 Hz (0.55 ppm) with ^{1}H decoupling and 121 Hz (0.60 ppm) without. Line widths for the same subset of Cα carbons for a different perprotio CN-ubq sample were extracted from a ^{1}H decoupled ^{13}C−^{13}C correlation spectrum reported on previously.[13] Under these conditions the ^{13}C line width is statistically identical to those observed with the ilvD-ubq sample at 118

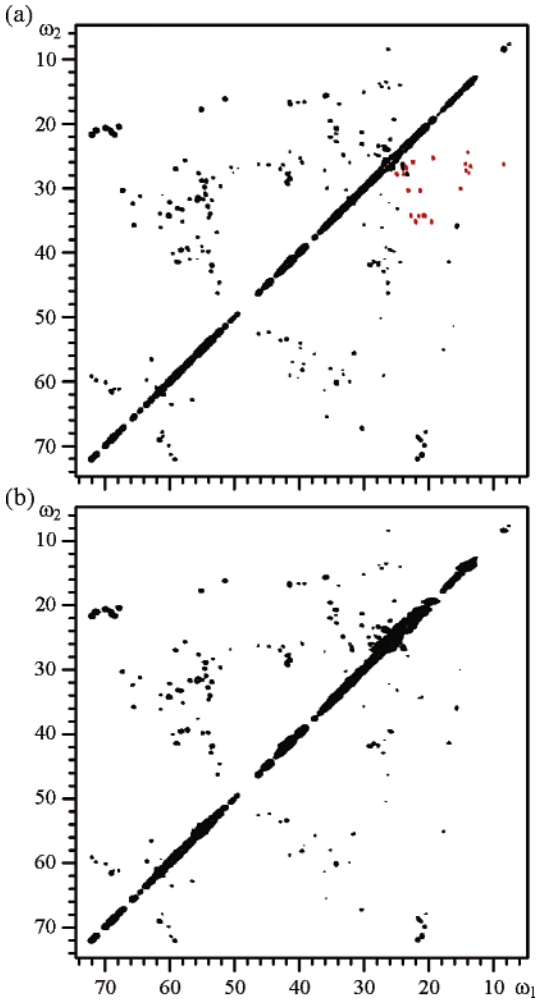

Figure 7. ^{13}C homonuclear RFDR spectra of ilvD-ubq. Spectrum (a) was taken with 100 kHz TPPM ^{1}H decoupling during both t_1 and t_2. The spectrum contains 1536 points in t_2 and 3072 complex points in t_1, each with a 100 kHz spectral window, for a total acquisition time of 15.36 ms in each dimension. 16 scans were collected per t_1 increment (14 h acquisition). Spectrum (b) was taken without decoupling during t_1 and with 1024 points in t_1 ($t_{1max} = 10.24$ ms). With 8 scans per t_1 increment data acquisition was 4.7 h. Each dimension was zero-filled to 4096 points and apodized with an identical slightly shifted cosine bell function. The cross-peaks that appear on only one side of the diagonal in the experiment with no ^{1}H decoupling during t_1 are shown in red.

(24) Bennett, A. E.; Ok, J. H.; Griffin, R. G.; Vega, S. *J. Chem. Phys.* **1992**, *96*, 8624−8627.
(25) Detken, A.; Hardy, E. H.; Ernst, M.; Meier, B. H. *Chem. Phys. Lett.* **2002**, *356*, 298−304.
(26) Hing, A. W.; Vega, S.; Schaefer, J. *J. Magn. Reson.* **1992**, *96*, 205−209.

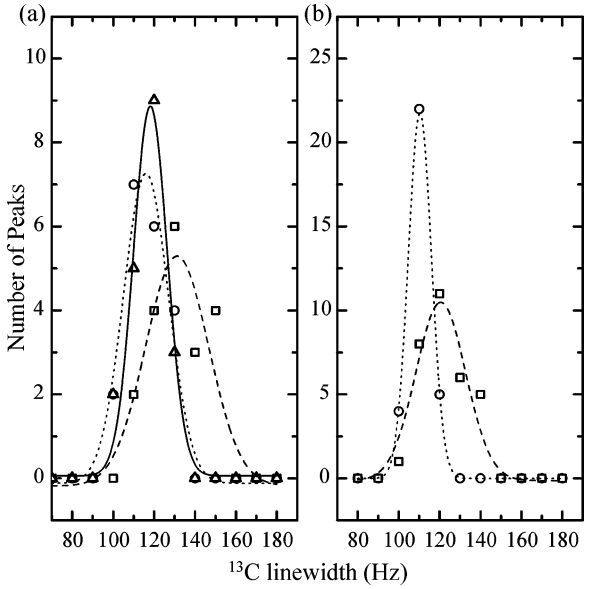

Figure 8. ^{13}C line width distributions observed for (a) 19 Cα and (b) 31 CO resonances. Results for the ilvD-ubq sample were extracted from ^{13}C−^{15}N two-dimensional correlation spectra. The squares and dashed line are ilvD-ubq data taken without ^{1}H decoupling during the ^{13}C detection, while the circles and dotted line are data acquired with 100 kHz XiX ^{1}H decoupling. The data were zero-filled once, and no apodization was applied. The ^{13}C detection periods were 15 ms in duration. The triangles and solid line in part (a) are data for a perprotio CN-ubq sample extracted from a two-dimensional ^{13}C−^{13}C homonuclear correlation spectrum with 90 kHz of TPPM decoupling applied during the ^{13}C evolution of 20 ms. These data were zero-filled once, and no apodization was applied. The same subset of 19 Cα peaks was chosen for this comparison. The full widths at half-height of the peaks were binned into 0.10 ppm bins, and the resulting distributions were fit to Gaussians.

Hz (0.59 ppm). Only a portion of the same subset of lines have sufficient signal-to-noise to have their line widths reliably measured from the lower signal-to-noise ^{13}C−^{13}C correlation spectrum shown in Figure 7a. For this reduced set an average of 100 Hz is obtained, and given the larger uncertainty this is judged to be within the error bar of the other measurements just described.

Two conclusions immediately follow from these results. The first is that there is not a statistically significant increase in ^{13}C line widths for the deuterated sites even though ^{2}H decoupling has not been applied. On average the deuterium substituted ^{13}Cα resonances are the same width as their protio counterparts within the estimated error of this measurement (±10 Hz). While we would predict some broadening due to the one bond J_{CD} scalar couplings, this is apparently a small effect. Figure 9 provides some insight as to why this is the case, depicting line shape simulations assuming $J_{CD} = 21$ Hz and coupling to two adjacent ^{13}C nuclei with $J_{CC} = 45$ Hz. The multiplet structure shown is then convoluted with a 50 Hz Lorentzian to account for the line width typically observed in ^{13}C CPMAS spectra of natural abundance samples such as that shown in Figure 1a. If these simulated line shapes are fit to Lorentzian profiles we obtain effective line widths in (a) of 100 Hz where $J_{CD} = 0$ Hz, and in (b) of 109 Hz where $J_{CD} = 21$ Hz. Deuteration is then expected to lead to an increase in ^{13}C line width of only ∼9 Hz from J_{CD}, a difference apparently too small to detect within the precision of the full width at half-maximum measurements reported on here.

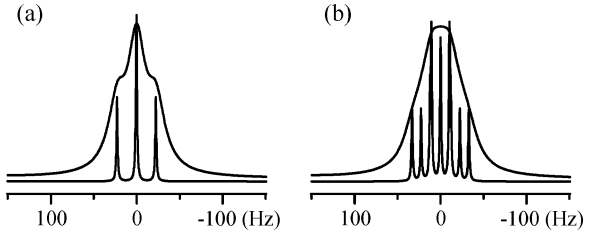

Figure 9. Simulated line shapes for Cα ^{13}C resonances with (a) ^{13}C scalar couplings to two neighboring ^{13}C atoms and (b) also ^{2}H scalar coupling to a single ^{2}H. The scalar couplings are assumed to be 45 Hz for J_{CC} and 21 Hz for J_{DC}. The narrow lines display the multiplet structure. The broadened envelope is what is expected based on inclusion of a Lorentzian broadening of 50 Hz which corresponds to the limiting line widths observed in the n-ubq ^{13}C spectrum shown in Figure 1a where there are no scalar couplings.

The second significant conclusion to be drawn from these data is that, for deuterated protein, ^{1}H decoupling is not strictly necessary in experiments where CO and deuterated Cα resonances are to be observed. For backbone resonance assignment using NCACO and NCOCA experiments,[7] this provides a significant advantage to perdeuterated proteins. The resolution that can be obtained for a perprotio sample for many proteins will be limited by the total length of the decoupling periods required for the ^{15}N and ^{13}C evolution. If decoupling can be dispensed with altogether for the ^{13}C dimensions, it can be reserved for ^{15}N evolution, potentially permitting higher resolution spectra to be acquired without risk of damaging the sample.

Conclusions

Potential problems with applying ^{13}C CPMAS NMR to extensively deuterated proteins have been shown to be inconsequential using ubiquitin as a test case. CP enhancements are found to be better than expected from exchangeable protons alone, and neither ^{1}H nor ^{13}C T_1 values are significantly lengthened. Given the reasonable ^{13}C T_1 values observed, a significant improvement in CP performance was obtained using a spinlock-CP sequence. This signal enhancement was retained in a spinlock-RADCP method introduced to also provide more even equilibration of ^{13}C magnetization among the CO, Cα, and side chain carbon centers in uniformly ^{13}C enriched material. At our field strength, deuterium decoupling is not found to be required, as the ^{1}H decoupled ^{13}C line widths are found to be experimentally indistinguishable for both perprotio and perdeutero material.

Deuteration is also found to provide significant advantages in many applications. By employing deuteration the ^{13}C resolution in 2D and 3D experiments need not be limited by decoupler heating. If ^{1}H decoupling is not applied, the CO and deuterated Cα carbon line widths only increase by a modest 0.08 ppm at a MAS rate of 20 kHz. Since deuteration also provides for very high resolution in the amide ^{1}H spectrum, this aspect can be taken advantage of in ^{1}H/^{15}N/^{13}C triple resonance experiments where the ^{1}H decoupling is critical for optimizing the ^{15}N resolution. Proteins that prove too sensitive to decoupler heating to be studied by the standard CPMAS methods may also prove accessible with extensive deuteration.

Dilution of the ^{1}H pool by deuteration was also found to shed insight into the relaxation dynamics of both the ^{1}H and ^{13}C spin reservoirs. The present data suggests that preferential sequestering of molecular oxygen in the hydrophobic portion of the protein may be a plausible source for short ^{1}H T_1 values that

are relatively insensitive to deuteration and the very rapid ^{13}C T_1 relaxation for a fraction of the side chain resonances. Further investigation of spin relaxation in nanocrystalline proteins in this vein is needed, and such studies will be expected to provide unique information on the dynamics of small molecules such as water and oxygen in the protein lattice.

Few barriers have been found in ^{13}C CPMAS experiments on a heavily deuterated protein, while several advantages have emerged. The convenience of being able to apply the entire suite of resonance assignment methods to the preferred sample for determining $^1H-^1H$ distance constraints is expected to make extensively deuterated material an attractive option for ssNMR studies of protein structure and function.

Acknowledgment. This work was supported in part by the W. M. Keck foundation, Yale University, and grants from the National Science Foundation. C.R.M. acknowledges the Natural Sciences and Engineering Research Council of Canada for a Post-Graduate Fellowship and Van Phan for assistance with the ^{13}C line width data.

JA045581X